Development of 10 kA Current Leads Cooled by a Cryogenic Mixed-Refrigerant Cycle

IOP Conf. Series: Materials Science and Engineering **502** (2019) 012138 doi:10.1088/1757-899X/502/1/012138

Development of 10 kA Current Leads Cooled by a Cryogenic Mixed-Refrigerant Cycle

Eugen Shabagin[1], **Steffen Grohmann**[1,2]

[1] Karlsruhe Institute of Technology (KIT), Institute of Technical Physics, Hermann-von-Helmholtz-Platz 1, 76344 Eggenstein-Leopoldshafen, Germany

[2] Karlsruhe Institute of Technology, Institute of Thermodynamics and Refrigeration, Engler-Bunte-Ring 21, 76131 Karlsruhe, Germany

E-mail: eugen.shabagin@kit.edu

Abstract. Current leads used to supply electrical energy from a room-temperature power supply to a superconducting application represent a major thermal load and therefore largely determine the operating cost. This paper presents a concept to minimize the thermal load at the cold end by integrating the recuperative heat exchanger of a cryogenic mixed-refrigerant cycle (CMRC). A mixture of non-flammable components is used to absorb the distributed thermal load continuously over the entire temperature range. The paper describes the numerical model that consists of an electric model coupled with a thermal modelling framework, allowing the optimization of the mixture composition and the temperature profiles. Simulations yield a reduction of the thermal load at the cold end by 45 % compared to conventional conduction-cooled current leads.

1. Introduction

Current leads transport electrical energy from room-temperature to a superconducting application at the cryogenic temperature and represent a major thermal load into the cryostat. The main contributions to the heat load are the ohmic heating $\dot{Q}_{\mathrm{el}}$ due to internal dissipation in the current lead and the heat conduction $\dot{Q}_{\mathrm{w}}$ from the warm terminal to the cold end. Both contributions have to be balanced by the selection of an appropriate geometry. In an optimized current lead, heat input from the warm terminal must be close to zero, yielding an adiabatic boundary condition [1]. This optimization minimizes the overall heat load $\dot{Q}_{\mathrm{c}}$ into the cold end, and the main contribution to the thermal load is reduced to ohmic heating.

Depending on the cooling method, the current lead can be classified into conduction-cooled or gas-cooled. Conduction-cooled current leads [1] are used in cryogen-free cryostat systems working with one cold stage, yielding the highest heat leak compared to other cooling options. The heat leak can be reduced by the application of several cooling stages [2–5] at intermediate temperatures (multi-stage cooled current lead). Gas-cooled current leads [6–9] require forced vapour flow for additional convective cooling, where the coolant is heated up in counter-flow to room-temperature. Combinations of the cooling methods [10], the use of Peltier elements [11] and the integration of high temperature superconductors [12] are further possibilities to reduce the heat leak.

In this paper, the calculation model of a cooling method is described, where the recuperative heat exchanger of a closed Joule-Thomson cycle is combined with a 10 kA current lead. The

use of a mixed (rather than a pure) refrigerant has been identified [13, 14] as an advantageous cooling method for current leads due to the thermodynamic benefit of absorbing heat over a broad temperature range [13–19]. In addition, the system is working at low operating pressures and minimal temperature differences in the recuperative heat exchanger due to two-phase heat transfer. The mixture consists of four non-flammable refrigerants (R14, R23, R218, R740), whereby R218 is the highest-boiling and R740 the lowest-boiling component. The fluid properties are calculated in Aspen Plus [20] with the Peng-Robinson equation of state [21] and binary interaction parameters from [22] down to a temperature of 120 K. Properties of non-flammable mixtures below 120 K are not yet available but will be investigated in the future [23]. As an intermediate solution, an additional cooling stage at 77 K is used in the model.

2. Current lead design

A cryogenic mixed-refrigerant cooled current lead (CMRC-CL) is shown in figure 1. The cold end is cooled by a cryocooler or liquid nitrogen to 77 K. In addition, the counter-flow heat exchanger (CFHX) of a Joule-Thomson cycle is part of the current lead, where the high pressure (HP) and low pressure (LP) streams are circulating. The LP stream cools the HP stream and the current lead continuously over the temperature range from 300 to 120 K. The first part of the current lead, that is connected with the CFHX, is $L_1 = 1.0$ m long. The length of the second part, from 120 K to 77 K, is $L_2 = 0.28$ m. A shorter connection to the cold stage at 77 K would lead to a temperature decrease of the mixture and imply a risk of freeze-out.

The CMRC-CL geometry is presented in figure 2, showing a segment of the current lead at the warm end. It is made of a cylindrical cooper rod with a residual resistance ratio of RRR = 50, with a milled rectangular helical groove for the heat exchanger. A quadratic Cu-profile with circular hole is brazed into the groove as cooling channel for the LP stream. The channel contains four stainless steel capillaries for the HP stream. The diameter D_i of the recess in the middle of the current lead can be adapted depending on the design amperage. For currents lower than 10 kA, the diameter has to be larger and vice versa.

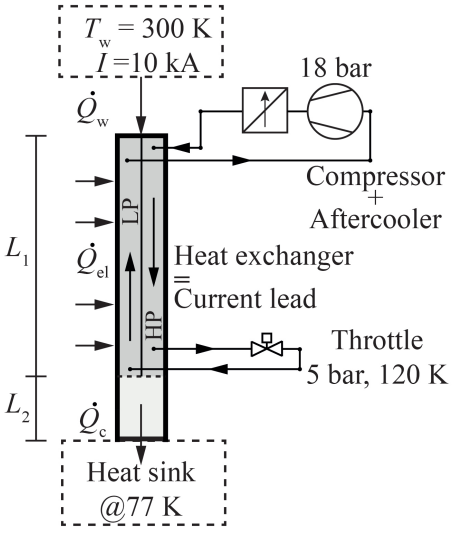

Figure 1. Schematic view of a cryogenic mixed-refrigerant cooled current lead.

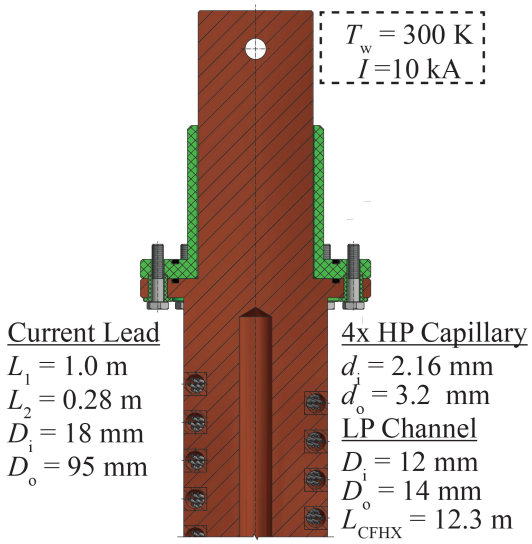

Figure 2. Segment of the conceptual design of the current lead at the warm end with integrated heat exchanger of a Joule-Thomson cycle.

3. Numerical model

The calculation of the temperature profile of the current lead $T_{\mathrm{CL}}(x)$ is performed based on the one-dimensional differential heat equation of second order:

$$\frac{\partial}{\partial x} \cdot \left(\lambda_{\mathrm{Cu}}(T_{\mathrm{CL}}) \cdot A \cdot \frac{\partial T_{\mathrm{CL}}}{\partial x} \right) + I^2 \cdot \frac{\rho_{\mathrm{Cu}}(T_{\mathrm{CL}})}{A} - \alpha_{\mathrm{LP}} \cdot U \cdot (T_{\mathrm{CL}} - T_{\mathrm{LP}}) = 0, \tag{1}$$

where λ_{Cu} is the copper heat conductivity, A the cross-section area, I the amperage, ρ_{Cu} the electrical resistivity, α_{LP} the heat transfer coefficient between the current lead and the LP stream and U the wetted perimeter. Fixed temperatures at the warm end $T_{\mathrm{CL,x=0}} = 300$ K and the cold end $T_{\mathrm{CL,x=L1}} = 120$ K are used as boundary conditions.

The temperature of the LP stream T_{LP} is found by modelling the heat exchanger with the numerical solution algorithm from [24]. This versatile model is capable of calculating the two-phase heat transfer and pressure drop of the HP and LP streams under consideration of axial conduction in the wall and in the fluid, parasitic heat loads and fluid property variation. The heat transfer coefficient α_{LP} shown in figure 3 is taken from [25], where existing correlations for boiling and condensation are modified, yielding an improved prediction of available experimental data.

The modelling of the heat exchanger/current lead is done in Mathematica [26]. The explicit Runge-Kutta method is used for the calculation of the temperature change and pressure drop of the HP and LP streams. Equation 1 is solved using the Finite-Difference-Method (FDM) with the Control-Volume approach and the Gauss-Seidel iteration [27]. Both methods are implemented in the iterative calculation loop explained in [24].

The preliminary extension of the current lead from L_1 with the length L_2 is modelled with the analytical expression in equation 2 for a conduction-cooled current lead with the boundary temperatures 120 K and 77 K and the heat load $\dot{Q}_1$ flowing from the upper part at $x = L_1$:

$$\dot{Q}_{\mathrm{c}} = \sqrt{{\dot{Q}_1}^2 + 2 \cdot I^2 \int_{77\mathrm{K}}^{120\mathrm{K}} \rho_{\mathrm{Cu}}(T) \cdot \lambda_{\mathrm{Cu}}(T) \mathrm{d}T}. \tag{2}$$

With equation 2 and Fourier's Law, it is possible to calculate the optimal geometry of the current lead and its temperature profile, which is shown in the next chapter.

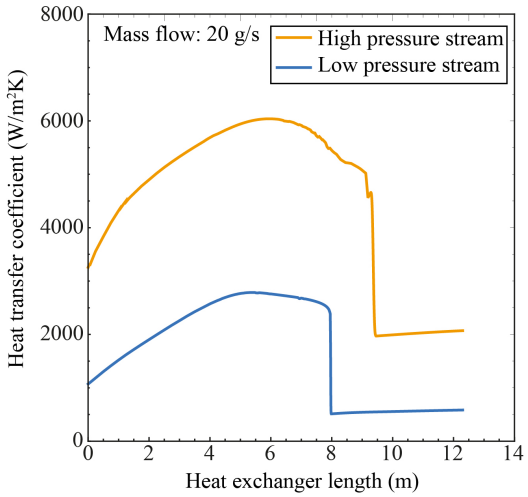

Figure 3. Heat transfer coefficients α_{HP} and α_{LP} of the HP and LP streams as a function of the heat exchanger length $L_{\mathrm{CFHX}} = 12.3$ m. The mass flow of the mixture in the Joule-Thomson cycle is 20 g/s. The molar mixture composition is R14=15 %, R23=15%, R218=35 %, R740=35 %.

4. Results

The temperature profiles in the heat exchanger/current lead as a function of the current lead length are shown in figure 4. The upper part of the current lead with the length L_1 includes the recuperative CFHX with the temperatures of the HP stream, the LP stream and the intermediate wall temperature. Temperature differences between the two streams varying along the length but are mainly around 8 K, only reaching 25 K in the warm region at the length coordinate 0.35 m. Between the current lead and the LP stream, the temperature difference is about 1 K and has two pinch points near the cold end. The pressure drop of the HP stream is relatively high with $\Delta p_{\mathrm{HP}} = 10.5$ bar; the LP stream pressure drop is $\Delta p_{\mathrm{LP}} = 2.2$ bar. Further design improvements in order to minimize the overall entropy production may further improve the performance.

Figure 5 compares the temperature profile of the cryogenic mixed-refrigerant cooled current lead CMRC-CL (3) with an optimized conduction-cooled current lead CC-CL (1) and a profile (2) corresponding to the absolute minimum heat load at the cold end of $\dot{Q}_{\mathrm{c},(2)} = 8.5$ W/kA under the theoretical assumption of an infinite number of Carnot stages along the length [28]. The goal of a current lead optimization is to lower the temperature gradient at the warm end close to zero, and to minimize the heat conduction $\dot{Q}_{\mathrm{w}}$ and therefore the heat load $\dot{Q}_{\mathrm{c}}$. The warm end goal is achieved in the temperature profiles (1) and (2), but not in the CMRC-CL profile. However, the CMRC-CL curve is showing characteristics similar to the theoretical curve (2) and could be further influenced by the mixture composition, and/or modification of the geometry at the warm end. Nevertheless, the heat load at the cold end of $\dot{Q}_{\mathrm{c},(3)} = 23.8$ W/kA yields a reduction of the thermal load by 45 % compared to conventional conduction-cooled current leads (1). This can be directly deduced from the temperature gradients at the cold end.

It is found that in order to minimize the heat load $\dot{Q}_{\mathrm{c}}$, the heat transfer area ($U \cdot L_{\mathrm{CFHX}}$) must be large and the current lead becomes relatively long. Therefore, another optimization goal should be the design of more compact current leads. This result gives a strong motivation for the development of micro-structured CFHX [29] and their integration in a current lead.

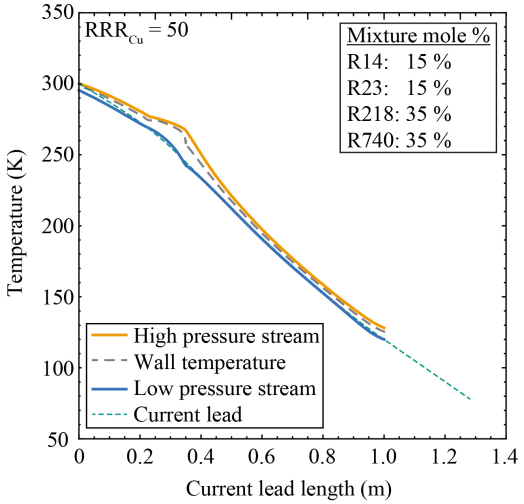

Figure 4. Temperature profiles of the cryogenic mixed-refrigerant cooled current lead.

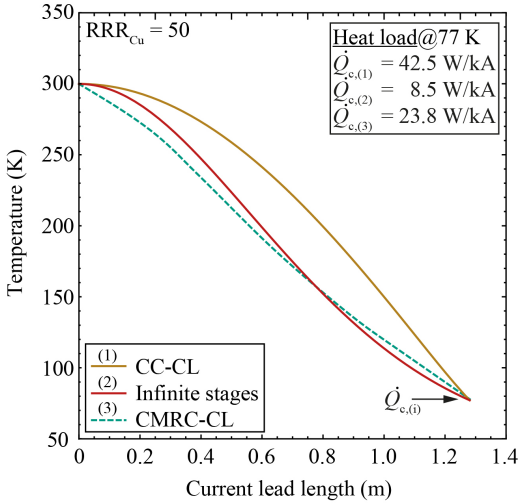

Figure 5. Temperature profile of the cryogenic mixed-refrigerant cooled current lead CMRC-CL in comparison with two different cooling methods.

5. Summary and conclusion

The results of numeric coupling of an electric model with a thermal modelling framework for the integrated optimization of a cryogenic mixed-refrigerant cooled current lead are presented in this work, using the design example of a 10 kA current lead for superconducting applications. This cooling method represents an efficient alternative to state-of-the-art solutions that require multiple stages, yielding a reduction of the thermal load at the cold end by 45 % compared to conventional single-stage conduction-cooled current leads. Verification of the model is performed by the adherence of the residuals of temperature convergence in the heat exchanger $res_{\mathrm{CFHX}} < 10^{-5}$ and in the current lead $res_{\mathrm{CL}} < 10^{-7}$. Further, the consistency of the model is verified with regard to energy conservation, yielding a numerical error as low as 1.5 %.

The results show that a large heat transfer area is required to minimize the thermal load, yielding relatively long current leads. Therefore, the tubes-in-tube design should be reconsidered in favour of the development of micro-structured counter-flow heat exchangers [29].

References

[1] McFee R 1959 *Rev. Sci. Instrum.* **30** 98-102; doi:10.1063/1.1716499.
[2] Jeong S and Smith J.L 1994 *Cryogenics* **34** 929-33; doi:10.1016/0011-2275(94)90078-7.
[3] Bromberg L, Michael P C , Minervini J V, and Miles C 2010 *AIP Conf. Proc.* **1218** 577-84; doi:10.1063/1.3422405.
[4] Yamaguchi S, Emoto M, Kawahara T et al. 2012 *Physics Procedia* **27** 448-51; doi:10.1016/j.phpro.2012.03.508.
[5] Schreiner F, Gutheil B, Noe M et al. 2017 *IEEE Trans. Appl. Supercond.* **27** 4802405; doi:10.1109/TASC.2017.2655108.
[6] Efferson K R 1967 *Rev. Sci. Instrum.* **38** 1776-79; doi:10.1063/1.1720670.
[7] Chang H M, Choi Y S, Van Sciver S W and Miller J R 2004 *AIP Conf. Proc.* **710** 944-51; doi:10.1063/1.1774775.
[8] Jiahui Z, Juntao T, Ming Q et al. 2010 *IEEE Trans. Appl. Supercond.* **20** 1705-09; doi:10.1109/TASC.2010.2040949.
[9] Ma J, Liu R and Zhang H 2010 *ICEMS* 1813-17.
[10] Yamaguchi S, Emoto M., Yamamoto N et al. 2013 *IEEE Trans. Appl. Supercond.* **23** 4802304; doi:10.1109/TASC.2013.2243896.
[11] Yamaguchi S, Takita K and Motojima O 1996 *ICEC/ICMC Proc.* **16** 1159-62.
[12] Chang H M and Van Sciver S W 1998 *Cryogenics* **38** 729-36; doi:10.1016/S0011-2275(98)00043-5.
[13] Nellis G F, Pfotenhauer J M and Klein S A 2004 *ASME Int. Mechanical Engineering Congress and Exposition* 339-46; doi:10.1115/IMECE2004-60284.
[14] Pfotenhauer J M, Pettitt J F, Hoch D W and Nellis G F 2006 *Cryocoolers* **14** 443-452.
[15] Venkatarathnam G 2008 *Cryogenic mixed refrigerant processes* Int. cryogenics monograph series (New York: Springer).
[16] Alexeev A, Haberstroh Ch and Quack H 2000 *Adv. Cryog. Eng.* **45** 307-314.
[17] Alexeev A, Haberstroh Ch and Quack H 2002 *Cryocoolers* **10** 475-79; doi:10.1007/0-306-47090-X_56.
[18] Kochenburger T M, Grohmann S and Oellrich L R 2015 *Physics Procedia* **67** 227-32; doi:10.1016/j.phpro.2015.06.039.
[19] Narayanan V and Venkatarathnam G 2019 *Cryogenics* **78** 66-73; doi:10.1016/j.cryogenics.2016.06.012.
[20] Aspen Technology 2014 Aspen plus v8.6.
[21] Peng D Y and Robinson D B 1976 *Ind. Eng. Chem. Fundamen.* **15** 59-64; doi:10.1021/i160057a011.
[22] Kochenburger T M 2018 Ph.D. thesis Karlsruhe Institute of Technology (KIT).
[23] Tamson J, Stamm M and Grohmann S 2018 *ICEC-ICMC Proc.* **27**.
[24] Gomse D, Kochenburger T M and Grohmann S 2018 *J. Heat Transfer* **140** 051801; doi:10.1115/1.4038852.
[25] Gomse D and Grohmann S 2018 *ICEC-ICMC Proc.* **27**.
[26] Wolfram Research 2017 Mathematica 11.2.0.0 Wolfram Research Inc. Campaign IL.
[27] Özisik N M 1993 *Heat Conduction* 2nd ed. (New York: John Willey & Sons).
[28] Hilal M 1977 *IEEE Trans. on Magnetics* **13** 690-93; doi:10.1109/TMAG.1977.1059320.
[29] Gomse D, Reiner A, Rabsch G et al. 2017 *IOP Conf. Series: Materials Science and Engineering* **278** 012061; doi:10.1088/1757-899X/278/1/012061.

Acknowledgments

The authors would like to acknowledge the support from the Karlsruhe School of Elementary Particle and Astroparticle Physics: Science and Technology (KSETA).